Effects of Types of Fillers on the Molecular Relaxation Characteristics, Dynamic Mechanical, and Physical Properties of Rubber Vulcanizates

NABA K. DUTTA and D. K. TRIPATHY*

Rubber Technology Centre, Indian Institute of Technology, Kharagpur 721302, India

SYNOPSIS

The dynamic mechanical, and physical properties of bromobutyl rubber were investigated to determine the effect of particle size and of the structure of carbon black and silica. Filler loading was so adjusted that all the experimental compositions had the same hardness level. The results indicate that the type and loading of filler have no significant effect on the molecular relaxation transition. However, elastomer having a desirable storage modulus with low sensitivity to temperature change can be developed using filler with smaller particle size. Higher elongation at break, and better tensile strength, energy density at break, and fatigue life could be obtained by using finer particle or high structure black than with the low structure and higher particle size black. Finer particle size filler loaded systems exhibit pronounced strain dependence, higher thixotropic change, and delayed recovery in dynamic mechanical properties compared to that exhibited by large particle size filler.

INTRODUCTION

The effects of fillers on the mechanical properties of elastomers are of great interest primarily because fillers can be used very efficiently to enhance the physical properties. They also strongly influence the viscoelastic properties of elastomer compounds. The dynamic properties of elastomers filled with structured fillers are influenced by factors such as type of filler, volume fraction of filler, processing conditions, and strain history. The dynamic mechanical properties of rubber loaded with carbon black have been the subject of many investigations[1-14] because of their importance to the performance of the product, especially energy dissipation, skid resistance, and other properties of vehicle tires. However, most of these studies were conducted at room temperature and above[3-6,8] or using only one type of carbon black.[8,9]

Recently, Trexler et al.[15] have reported the effects of types of carbon black on the dynamic mechanical properties of elastomer over a temperature range of −40°C to +40°C. They made a comparison among fillers at equal volume loading. However, from the practical design point of view, comparison among the fillers seems to be more appropriate on the basis of property assessment.

Studies on dynamic fatigue life are of paramount importance since most of the rubber compounds are subjected to some form of fatigue loading. Fatigue to failure may be caused by flaws induced in service (ozone attack, mechanical cutting, etc.) or by flaws which were originally present in the sample. Fracture by crack formation is an irreversible kinetic process in the growth of flaws caused by some local inhomogeneity.[16] Rivlin and Thomas[17] have shown that the cut growth by catastrophic tearing is described by an energy criterion. From the fracture mechanics point of view (failure being essentially a cut growth process taking place from small flaws present in the test piece), and considering the tearing energy theory of Rivlin and Thomas,[17] Gent et al.[18] developed a mathematical relationship for gum natural rubber. In the tensile fatigue test, the fatigue life has been represented as

$$N = G/(2kW)^2 c_0 \quad (1)$$

where N = fatigue life in kilocycle; W = energy den-

* To whom correspondence should be addressed.

Journal of Applied Polymer Science, Vol. 44, 1635–1648 (1992)
 CCC 0021-8995/92/091635-14$04.00

sity at maximum extension ratio occurring during each cycle; G is the cut growth constant, which depends on polymer, filler type and loading, antidegradants used and other compounding variables and also on the vulcanizate structure; and k is a function of the extension ratio λ.

In a subsequent investigation, Lake and Lindley[19] derived the following equation for gum SBR vulcanizates,

$$N = G/3(2kW)^4 c_0^3 \quad (2)$$

Dizon et al.[20] extended the tearing energy concept to filled systems and observed an empirical relationship for filled SBR systems as follows:

$$N = G/3(2kW)^4 c_0 \quad (3)$$

In general, the equation may be written as

$$N = G/(n-1)(2kW)^n \cdot c_0^b \quad (4)$$

Greensmith[21] has determined k experimentally at various values of λ by purely elastic measurements, and reported that at extension ratios of 2 to 3, k is about 2 and not very sensitive to strain. The variable n is known as the strain exponent as it is the gradient of the fatigue curve obtained by plotting fatigue life, N, against strain energy density, W, on a double logarithmic plot; b is a numerical constant.

This investigation reports on the effects of different types of fillers (both black and nonblack) on the physical, dynamic, and mechanical properties and on the fatigue life characteristics of bromobutyl rubber over a wide range of experimental conditions. Compositions for different systems have been adjusted (by varying filler concentration) to attain equal hardness levels for all the systems. The effects of temperature, frequency and strain amplitude have been studied on the dynamic mechanical properties.

EXPERIMENTAL

Materials Used

Details of the formulation of the mixes are given in Table I.

Bromobutyl X_2 (BIIR) was manufactured by Polysar, Canada, and had density 0.93 g/cm^3, Mooney viscosity ML_{1+8} at 100°C = 55, and consisted of 1.8 wt % bromine. Zinc oxide was of chemically pure grade, specific gravity, 5.4. Stearic acid was of chemically pure grade. Paraffin oil was of pharmaceutical grade, specific gravity, 0.82. Sp-1045 is cure active phenolic formaldehyde resin obtained from Schenectady, Inc., USA, with specific gravity, 1.05, and melting point, 54°C.

Carbon Blacks

Conductive furnace black was Ketjan black-EC, manufactured by Akzo Chemical, Holland. Surface area, 950 m^2/g; DBP (dibutyl phthalate) adsorption, 360 mL per 100 g; pH 8.

The furnace blacks were supplied by Phillips Carbon Black Ltd., Durgapur, India. The designation and properties of the carbon blacks were as follows:

- SAF: Super abrasion furnace (N − 110); surface area, 142 m^2/g; DBP absorption, 112 mL/100 g; pH, 7.8.

Table I Composition in 100 Parts by Weight of Rubber Samples

	B_{CON}	B_{SAF}	B_{HAF}	B_{FEF}	B_{GPF}	B_{SRF}	B_{SIL}	B_{SIC}
BIIR	100	100	100	100	100	100	100	100
ZnO	5	5	5	5	5	5	5	5
Stearic acid	1	1	1	1	1	1	1	1
Paraffin oil	10	10	10	10	10	10	10	10
SP-1045	10	10	10	10	10	10	10	10
Ketjan EC	40	—	—	—	—	—	—	—
SAF	—	50	—	—	—	—	—	25
HAF	—	—	60	—	—	—	—	—
FEF	—	—	—	65	—	—	—	—
GPF	—	—	—	—	75	—	—	—
SRF	—	—	—	—	—	85	—	—
Silica	—	—	—	—	—	—	55	30
SI-69	—	—	—	—	—	—	5	3

Table II Curing Characteristics of the BIIR Vulcanizates

	B_{CON}	B_{SAF}	B_{HAF}	B_{FEF}	B_{GPF}	B_{SRF}	B_{SIL}	B_{SIC}
Mooney viscosity								
At 120°C, ML_{1+4}	79	50	49	45	49	50	120	80
Scorch time, min	9	11	13	30	25	23	6	6
Rheometer data								
At 160°C minimum viscosity	18	11	11	9	10	11	16	15
Scorch time, ts_2	5	3.5	3.5	4.0	4.0	4.0	2.75	2.75
Optimum cure time, min	33.5	18.0	18.5	18	18.5	19.5	43	39.5
Rate of cure	3.10	6.89	6.66	7.14	6.89	6.45	2.48	2.72

- HAF: High abrasion furnace (N − 330), surface area 80 m^2/g; pH, 7.6.
- FEF: Fast extrusion furnace (N − 550); surface area, 45 m^2/g; DBP absorption, 120 mL/100 g; pH, 7.8.
- GPF: General purpose furnace (N − 660); surface area, 35 m^2/g; DBP absorption, 91 mL/100 g; pH, 7.6.
- SRF: Semi-reinforcing furnace (N − 774); surface area, 32 m^2/g; DBP absorption, 72 mL/100 g; pH, 7.7.
- Silica: Ultrasil VN_3; manufactured by Degussa, West Germany; Surface area, 234 m^2/g; oil absorption, 240 g/100 g; pH, 6.0.

Sample Preparation Technique

The compounds were mixed in a laboratory size (325 mm × 150 mm) mixing mill at a friction ratio of 1 : 1.19 according to ASTM D3182, by careful control of temperature, nip gap, time of mixing and uniform cutting operation. In order to achieve the same hardness in all compounds, the range of filler loading was varied as shown in Table I. The temperature range for mixing was 75–80°C. The order and time period of mixing were as follows:

- 0–2 min—Mastication.
- 2–8 min—Addition of $\frac{1}{3}$ filler plus $\frac{1}{3}$ oil.
- 8–17 min—Addition of $\frac{1}{3}$ filler and $\frac{1}{3}$ oil.
- 17–20 min—Addition of remaining filler and oil.

Black master batches so prepared were kept for 24 h after which mixing of other ingredients was carried out as follows:

- 0–3 min—Addition of curatives (mill temperature 60°C).
- 3–4 min—Refining through tight nip gap and dump. The nip gap was 1.5 mm.

After mixing the elastomer compositions were molded in an electrically heated hydraulic press to the optimum cure (90% of the maximum cure) using molding conditions previously determined from torque data obtained by a Monsanto rheometer (R-100). Specimens for the Goodrich flexometer test

Table III Physical Properties of the BIIR Vulcanizates

	Hardness	Tensile Strength MPa	Modulus at 300% MPa	Elongation at Break, %	Heat Build-Up, °C	Dynamic Set, %	Strain Energy Density W_b J/cc	V_r
B_{CON}	65	14.5	7.5	530	35	5.2	36.12	0.3210
B_{SAF}	64	15.9	9.1	450	26	5.7	29.82	0.3045
B_{HAF}	65	12.7	12.2	350	25	5.8	18.66	0.3157
B_{FEF}	64	11.0	9.4	360	26	5.9	18.0	0.2939
B_{GPF}	64	10.6	9.9	330	26	6.1	16.98	0.2964
B_{SRF}	65	10.8	10.8	330	25	7.3	15.0	0.2865
B_{SIL}	65	15.4	5.4	560	22	5.6	35.28	0.3059
B_{SIC}	65	15.5	7.9	470	24	5.3	32.46	0.3197

were vulcanized for 10 min in excess of the optimum cure time.

Test Procedures

Physical Test Methods

Processing and curing characteristics of the compounded stocks were determined using a Mooney viscometer (ASTM D 1646-81) and an oscillatory disc rheometer (R-100) (ASTM D 2084-81). Modulus, tensile strength, and elongation at break were determined according to ASTM D 412–80 at 25°C using a dumbbell specimen punched out using type D die. Tear strength was determined according to ASTM D 624-81 (type C). Both tensile and tear tests were carried out using a Zwick tensile UTM-1445, at a cross-head speed of 500 mm per minute. Hardness was measured according to ASTM D 2240-81. A Goodrich flexometer conforming to ASTM designation D 623-78 (method A) was used to mea-

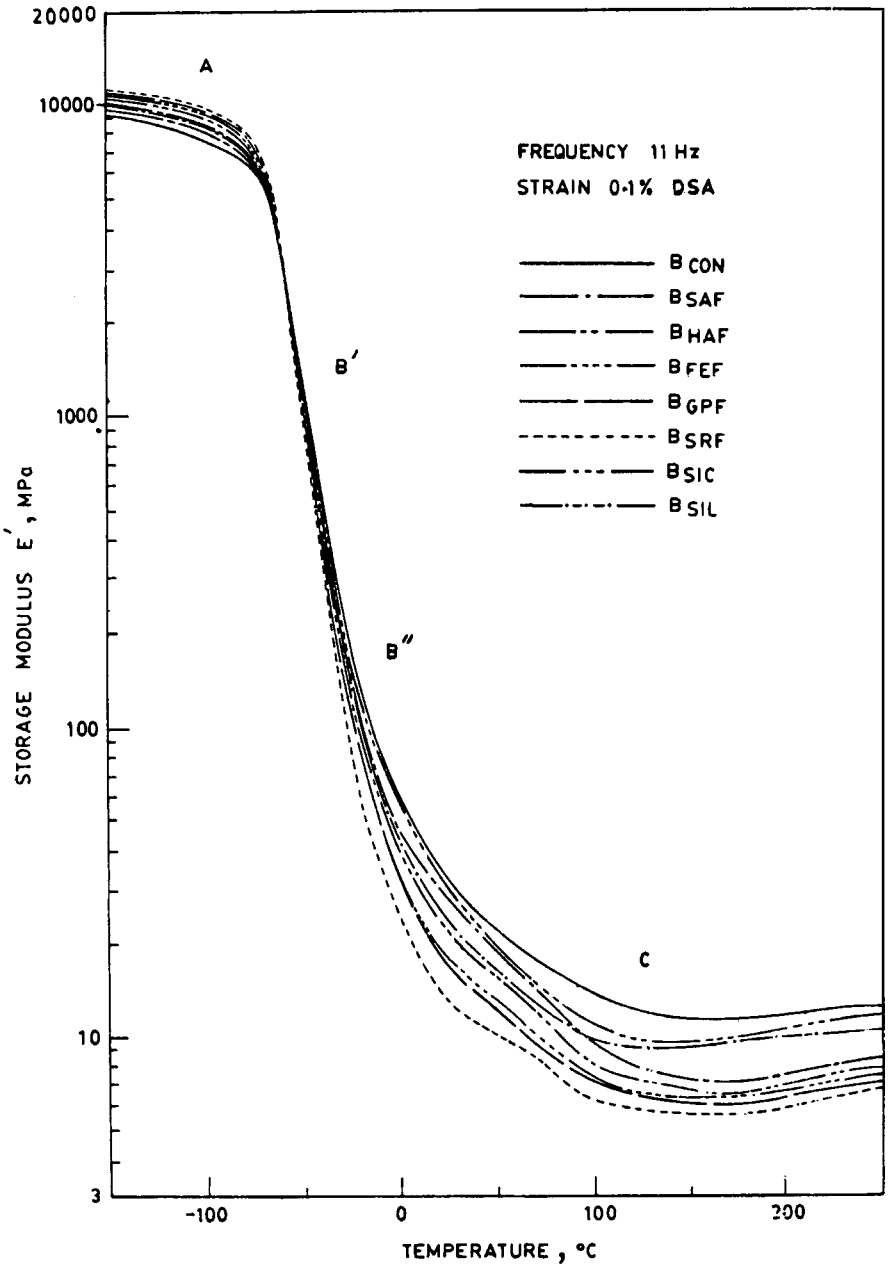

Figure 1 Effect of temperature on storage modulus for different filler loaded vulcanizates.

sure heat buildup and dynamic set after a specific dynamic flexing time.

Dynamic mechanical analysis was carried out using a viscoelastometer Rheovibron DDV-III-EP. The experiment was carried out in the tension mode over a temperature range of −150°C to +250°C with a programmed heating rate of 1°C/min, whenever results were scanned isochronally over a wide range of temperature. The general procedure was to cool the sample to −150°C, hold the sample at this temperature for 10 min and then record the measurements during warm-up. The experiment was performed isothermally over a wide frequency range. The dynamic strain amplitude was varied between 0.7×10^{-3} DSA (0.07% dynamic strain) to 50×10^{-3} DSA (5% dynamic strain). Double strain amplitude (DSA) refers to the ratio of peak to peak deformation, i.e. the total excursion path of the sample to the length of the sample ($2\ \Delta L/L$). Frequency range was 3.5 to 110 Hz. For a particular sample, the test was carried out first at the lowest available strain and later the strain was increased stepwise to the maximum.

To determine the thixotropic nature of the amplitude effect, the sample was vibrated initially at a strain amplitude of 0.5% DSA then subjected to a vibration at an amplitude of 5% DSA. The dynamic properties were measured as quickly as possible after the start of vibration and at intervals afterwards. The first value of the modulus at the higher strain was considerably lower than that obtained at the low amplitude. After 10 min vibration at higher amplitude the amplitude was reduced to the initial low value, and was measured again as quickly as possible and at intervals thereafter. The percentage recovery in dynamic properties (compared to the initial value) with respect to time is reported.

Determination of Volume Fraction of Rubber

The volume fraction of rubber V_r was determined by using the equilibrium swelling method. Samples of approximately 10 mm diameter, 2.5 mm thickness, and 0.3 g weight, were punched out from the central portion of the vulcanizates and allowed to swell in cyclohexane at 35°C in the thermostatically controlled water bath. Swollen sample were taken out after equilibrium swelling, blotted with filter paper, and weighed quickly in a stoppered weighing bottle. Samples were then dried in a vacuum oven for 24 h, at 70°C and finally weighed after being allowing to cool in a desiccator. Triplicate readings were taken for each sample. The V_r values were calculated using the method reported by Ellis and Welding.[22]

The equation used for calculating the V_r value is given by:

$$V_r = \frac{(D - F_0T)\,\rho_r^{-1}}{(D - F_0T)\,\rho_r^{-1} + A_0\rho_s^{-1}} \qquad (5)$$

where D = deswollen weight of the test specimen; T = initial weight of the test specimen; F_0 = weight fraction of the insoluble component in the sample; A_0 = weight of absorbed solvent, corrected for swelling increment; ρ_r = density of rubber; ρ_s^{-1} = density of the solvent.

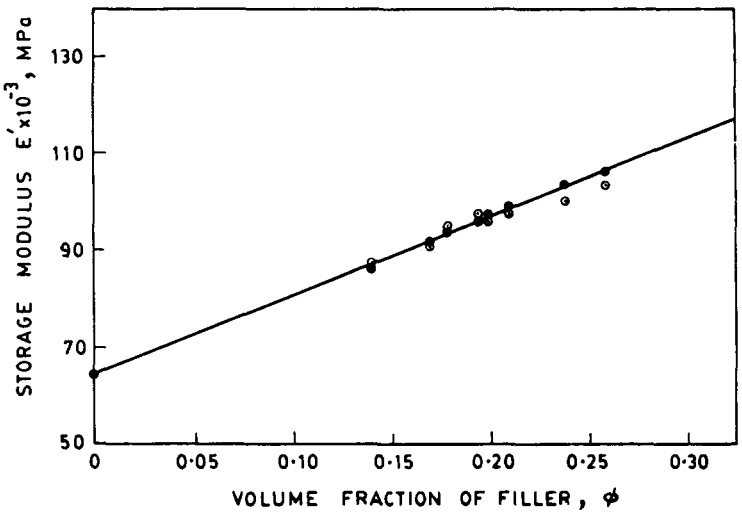

Figure 2 Effect of volume fraction ϕ of filler on storage modulus E' in the glassy state: ⊙ Experimental result; ● Calculated from Smallwood's equation.

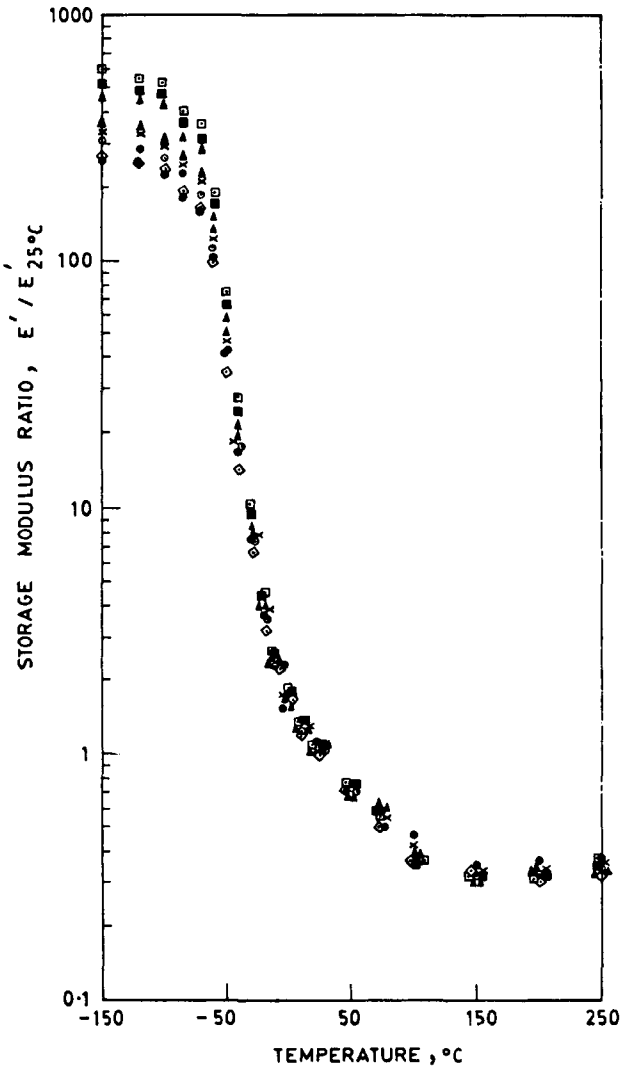

Figure 3 Relative storage modulus–temperature relationship for different filler loaded vulcanizates: ● B_{CON}; ⊙ B_{SAF}; ▲ B_{HAF}; ▲ B_{FEF}; ■ B_{GPF}; ⊡ B_{SRF}; × B_{SIL}; ◇ B_{SIC}.

RESULTS AND DISCUSSION

Curing Characteristics and Physical Properties

Curing characteristics and physical properties of the vulcanizates are given in Tables II and III respectively. Values of V_r have also been reported in Table III. The silica filled (B_{SIL}) system gives rubber stock with a very high Mooney viscosity. Among carbon black systems B_{CON} exhibits the highest viscosity. Finer particle blacks give scorchy stocks. The rates of cure of silica filled and conductive black filled systems (B_{SIL}, B_{SIC}, and B_{CON}) are found to be low. However, the rate of cure for other black loaded systems is comparable.

From Table III, it is evident that the compositions B_{CON}, B_{SAF}, B_{SIL}, and B_{SIC} show comparable strength properties. For other systems, the strength is found to be of the order of $B_{SAF} > B_{FEF} > B_{SRF} > B_{GPF}$. Better tensile strength, higher elongation, and higher energy density at break could be obtained by using finer particle or higher structure black at low loading than that with the low structure black at higher loading. Silica filled and silica–black combined systems exhibit properties equivalent to those of fine particle blacks. Among the vulcanizates, B_{CON} exhibits the highest heat buildup and B_{SIL} the lowest. Other vulcanizates have comparable values. Highly filled systems B_{GPF} and B_{SRF} show higher dynamic set. A marginally high V_r value is exhibited by highly active fillers, compared to weakly active fillers.

Effect of Temperature on Storage Modulus, E′

Figure 1 shows the storage modulus, E' for different vulcanizates over a temperature range of −150°C to +250°C. The characteristic sigmoidal variation of the storage modulus E' with temperature is apparent from the plot for all the compositions. It consists of three distinct regions. They are (A) glassy region, (B) transition region, and (C) rubbery region. In the glassy region, irrespective of the type of filler, particle size and structure, increased filler loading enhances the storage modulus value (E'). In Figure 2, E' was measured at very low temperature (−130°C), where the polymer is essentially in the glassy state; the values are plotted against the volume fraction (Φ) of filler loading. Experimentally obtained E' values follow a linear relation with Φ. Theoretically calculated values based on the Smallwood equation,[23]

$$E' = E'_0(1 + 2.5\Phi)$$

where E'_0 and E' are the moduli values for gum and filled systems, are also shown on the same plot. The agreement of the experimentally obtained value with the theoretically calculated value is excellent. Therefore, in the glassy region the increase in E' with filler loading is independent of the type, particle size, and structure of the filler and is only dependent on the volume fraction of filler loading. The augmentation in E' with filler loading can be attributed to the hydrodynamic effect of the filler particle embedded in the polymer continuum. Polymer filler interactions or filler aggregate–aggregate interactions, which have pronounced effect on E' value in the rubbery region of a polymer, have no significant influence in the glassy region. In the initial part of

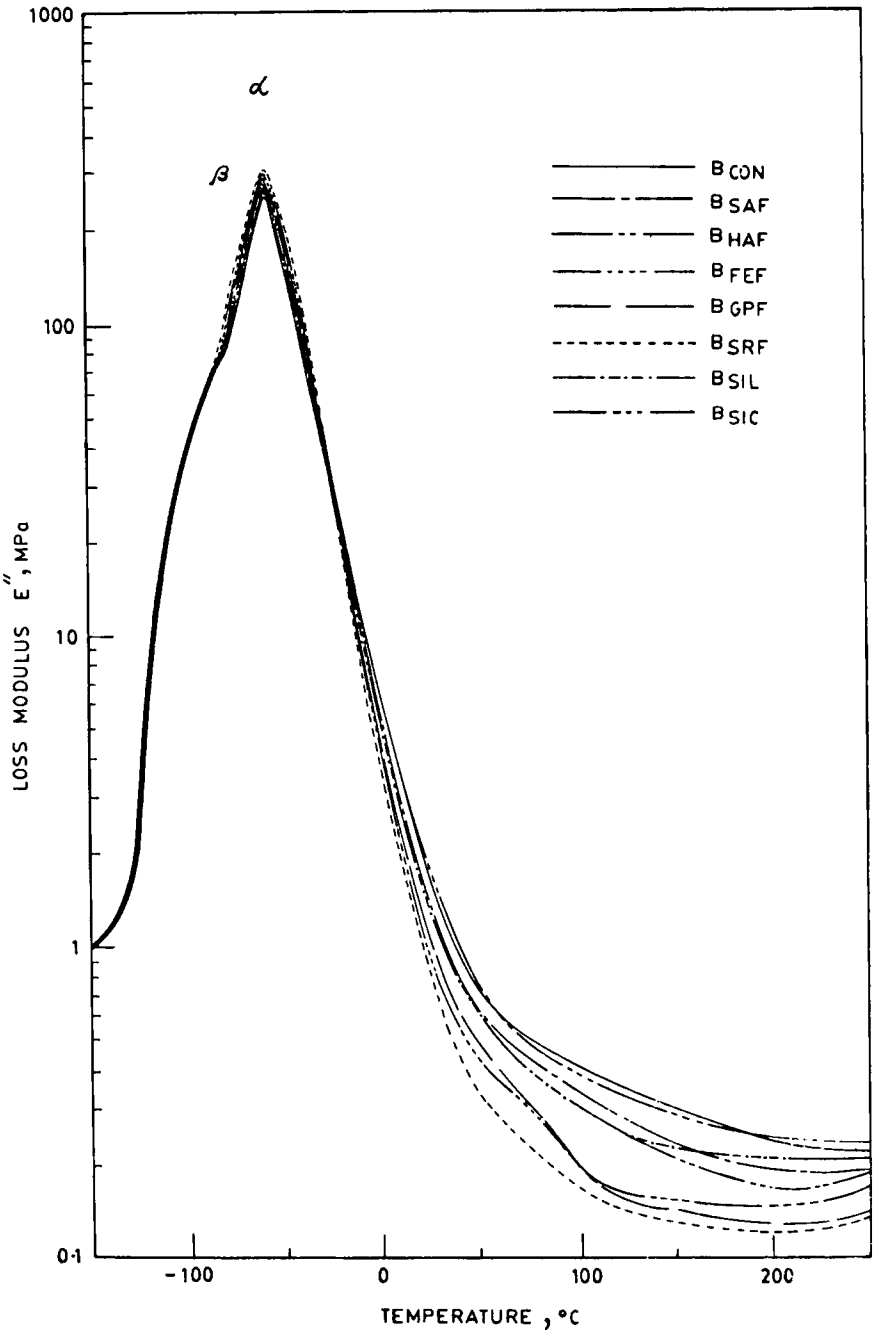

Figure 4 Effect of temperature on loss modulus for different filler loaded vulcanizates.

the transition region (B_1), the storage modulus values of all the vulcanizates are comparable. This is followed by a crossover region at the temperature range of −70°C to −60°C, above which a trend in E' opposite to that in the glassy state has been observed. In the rubbery region, the high-structure and finer-particle filler at low loading gives higher E' value than that with low-structure, larger-particle black at high loading.

Variation of the storage modulus with temperature for elastomeric composites is a very important design criterion. Lee[24,25] has pointed out that an elastomer composition with dynamic mechanical properties less sensitive to temperature change is required in order for automotive suspension systems to maintain ride comfort even at low temperature. In order to evaluate the temperature sensitivity of the modulus of elastomers, the term *relative storage*

Table IV Relaxation Transition Characteristics of Cured BIIR-Resin Compositions

	Loss Tan δ				Loss Modulus, E''			
	β Peak		α Peak		β Peak		α Peak	
	Temp °C (minus)	Value	Temp. °C (minus)	Value	Temp. °C (minus)	Value MPa $\times 10^{-2}$	Temp. °C (minus)	Value MPa $\times 10^{-2}$
B_{CON}	79	0.042	28.3	0.610	79	2.78	58.2	8.53
B_{SAF}	78.8	0.044	29.2	0.665	78.8	3.02	58.1	8.96
B_{HAF}	79.2	0.051	29.4	0.696	79.2	3.49	58	9.24
B_{FEF}	79	0.051	28	0.763	78.9	3.41	58.5	9.27
B_{GPF}	79	0.047	28.4	0.776	79	2.99	57.3	9.64
B_{SRF}	79	0.039	29	0.833	79	3.04	58.0	10.10
B_{SIC}	79	0.049	29	0.644	79	3.15	58	9.96
B_{SIL}	80	0.045	29.4	0.693	80	3.12	59	9.01

modulus, defined as the storage modulus at any temperature, $E'(T)$, divided by the storage modulus at room temperature, E' (25°C), is a useful parameter.[24,25] The relative storage modulus for all the composites has been calculated and is illustrated in Figure 3. So far as low temperature sensitivity is concerned, finer-particle black filled elastomer exhibits less sensitivity to temperature change. The low temperature sensitivity of the silica filled system (B_{SIL}) is comparable to that of finer particle black systems (B_{CON}, B_{SAF}). Silica-carbon black filled composition, (B_{SIC}) gives the best low temperature sensitivity among all the systems. However, higher temperature sensitivity is comparable for all the compositions.

Effect of Temperature on Loss Modulus, E''

Figure 4 represents the temperature dependence of E'' for the various compositions. For all the compositions, two distinct transition relaxation peaks are observed. They are designated as α and β relaxations respectively. Details about the magnitude and location of these peaks are given in Table IV. The low temperature transition (β transition) in the vicinity of −80°C may be attributed to the motion of the methyl groups directly attached to the backbone of BIIR.[26] The type of filler has no significant effect on the β peak location and intensity. The α peak is located in the transition region between the glassy state and the rubbery state. The type and loading of filler do not affect the $T^{\alpha}E''_{max}$ temperature; however, the intensity of α peak increases with increased loading of filler (irrespective of particle size and structure). The crossover point has been observed in the region of −50°C to −40°C. In the rubbery region, E'' also follows the same trend (E'' decreases with low structure filler) as observed in the case of storage modulus, E'.

Effect of Temperature on Loss Tangent, tan δ

Figure 5 shows the loss tangent spectra of the vulcanizates. As in E'' spectra, also two distinct transition relaxations are also reflected in tan δ spectra. The β transition occurs at about −80°C as observed in E'' spectra. However, a peak ($T^{\alpha}_{\tan\delta,\,max}$) in the spectrum is observed at about −29°C. This lies about 28°C above the a peak temperature observed in E'' ($T^{\alpha}_{E'',\,max}$) spectra. The $T^{\alpha}_{\tan\delta,\,max}$ peak location is not significantly affected by the filler concentration and types of fillers. The details about tan δ peak magnitudes and locations are given in Table IV. The tan δ peak magnitude is found to decrease with the use of more active fillers, ($B_{CON} < B_{SAF} < B_{HAF} < B_{FEF} < B_{GPF} < B_{SRF}$) although the volume loading is reduced. It is also evident from the figure that at higher temperature (far above $T^{\alpha}_{\tan\delta,\,max}$) high-structure filler loaded compositions show a broad maximum. Filled polymer constitutes a system with complex structure resulting in a different relaxation phenomenon which is absent in the gum vulcanizate.[27] The restricted mobility of the molecular segments resulting from strong surface adsorbtion forces will change the physical properties of the rubber near the particle surfaces, producing an encapsulating shell of higher rigidity (shell rubber) and having a higher $T^{\alpha}_{\tan\delta,\,max}$ temperature than the matrix rubber phase. This has been demonstrated by Smit,[27] and by Dutta and Tripathy[28] through dynamic mechanical analysis, and by Fujiwara et al.[29] and Kaufman et al.[30] through NMR studies. More

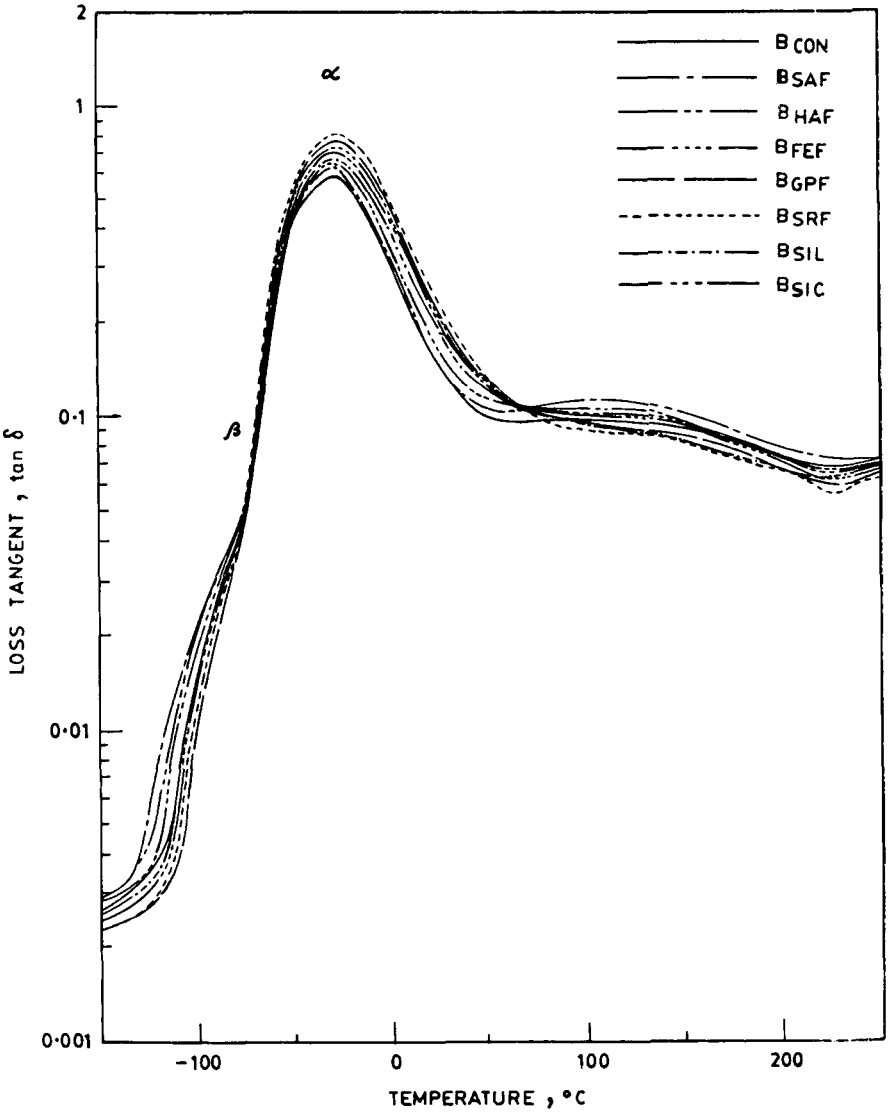

Figure 5 Effect of temperature on loss tangent for different filler loaded vulcanizates.

active filler surface should facilitate the formation of adsorbed shell formation and thus lower the tan δ peak intensity. BIIR filled with active fillers exhibits multiple relaxation phenomena in the highly elastic region (above $T^{\alpha}_{\tan\,\delta,\,\max}$) which may be ascribed to the segmental mobility in the interphasic layers of the adsorbed rubber hard shell surrounding the filler aggregate.

Effect of Dynamic Strain Amplitude

Figures 6 and 7 illustrate the storage modulus, E' and loss tangent, tan δ, for different vulcanizates, as a function of dynamic strain amplitude at 25°C and 11 Hz. The storage modulus decreases and tan δ increases with increasing amplitude. This is a familiar effect and can be explained on the basis of polymer–filler interaction,[1,31,32] desorption and reabsorption of hard rubber shell surrounding the filler aggregate,[27,28] or breaking and reforming of effective crosslinks in the rubber-forming transition zone between the bound rubber and the bulk rubber.[14] It is clearly observed from the figures that at equal hardness levels, different filler loaded vulcanizates exhibit different elastic moduli, loss tangents (hysteresis), and strain dependent characteristics (nonlinearity). The nonlinearity is less pronounced with higher particle size filler even at higher loading (e.g., B_{SRF} and B_{GPF}). However, a very pronounced effect is observed with low particle filler even at low

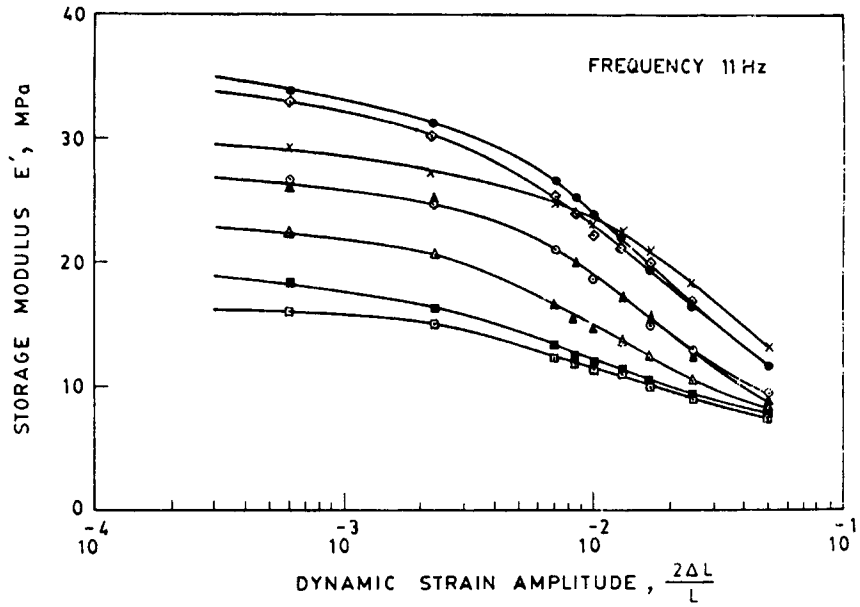

Figure 6 Storage modulus as function of dynamic strain. Key as Figure 3.

loading (B_{CON}, B_{SAF}, B_{HAF}, etc.). The difference in dynamic properties among the vulcanizates decreases with increasing strain amplitude. For example at 0.07% DSA, B_{CON} has E' value 120% higher than that of SRF black filled system (B_{SRF}). However, at 5% dynamic strain the B_{CON} system has E' value only 40% higher than that of B_{SRF}. On the other hand, at 0.07% DSA (B_{SRF}) has 150% higher tan δ value than that of B_{CON}, while at 5% DSA their tan δ values are comparable.

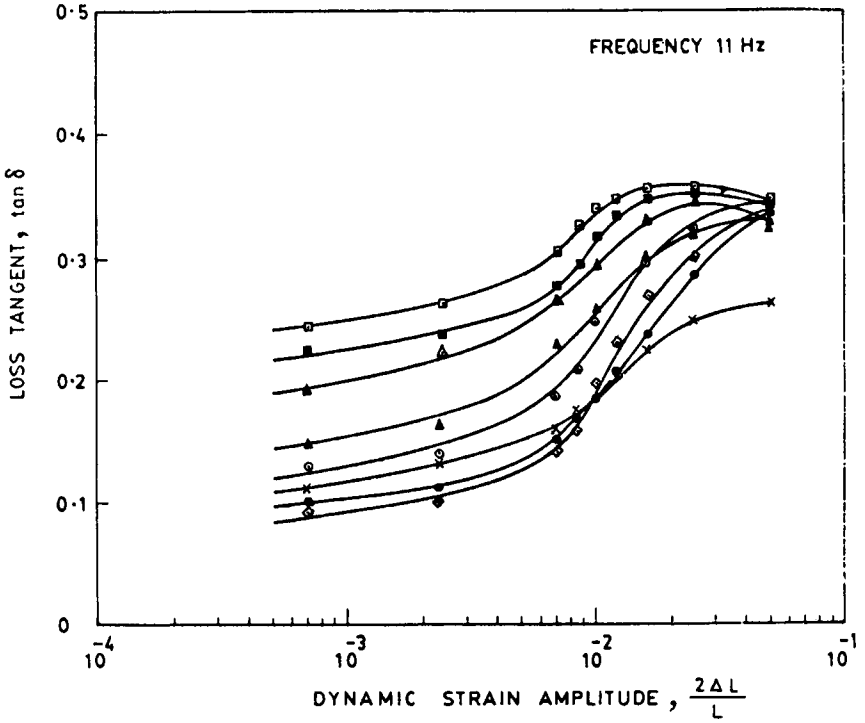

Figure 7 Loss tangent as function of dynamic strain. Key as Figure 3.

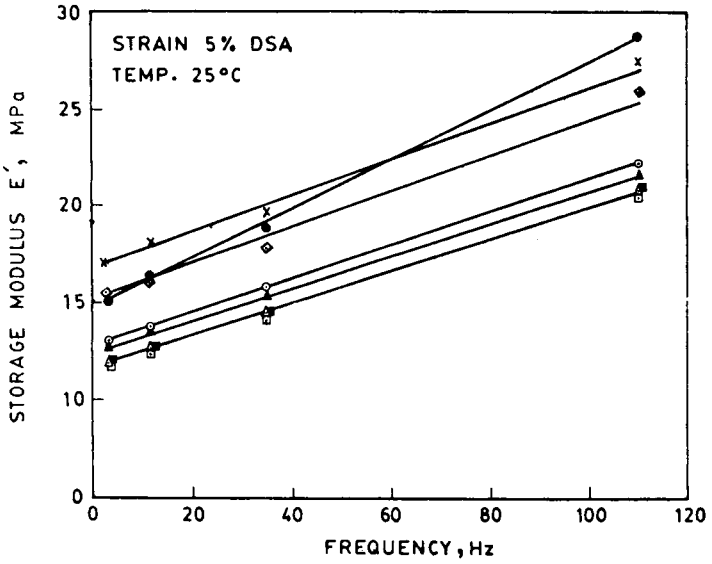

Figure 8 Effect of frequency on storage modulus. Key as Figure 3.

The silica filled system (B_{SIL}) shows relatively higher elastic modulus and lower tan δ compared to that of carbon black filled system (of similar surface area). Therefore, through proper choice of the type of filler, it is possible to adjust the loss tangent (and hysteresis) independent of the elastic modulus or related properties.

Effect of Frequency on Dynamic Properties

Figure 8 reflects the effect of frequency of vibration on E' for different vulcanizates at 5% DSA and 25°C. With increasing frequency, E' increases and follows a linear relationship for all the systems. The rate of frequency dependence (slope of the straight line) is comparable for all the vulcanizates, except B_{CON}. This composition has a higher sensitivity towards frequency.

Figure 9 illustrates the frequency dependence of tan δ for different compositions under similar conditions. For all the compositions, tan δ values follow a nonlinear relationship with frequency. Except B_{SIL}, all other compositions show comparable tan δ values up to 35 Hz. Silica filled system (B_{SIL}) shows lower value of tan δ. For very active filler loaded systems (B_{CON}, B_{SAF}), tan δ decreases as frequency increases from 35 Hz to 110 Hz, which may be accounted for by the excessive internal heat generation at higher frequency.

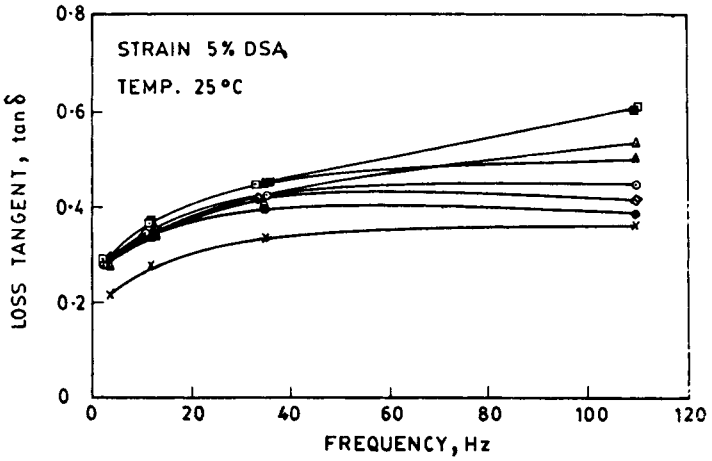

Figure 9 Effect of frequency on loss tangent. Key as Figure 3.

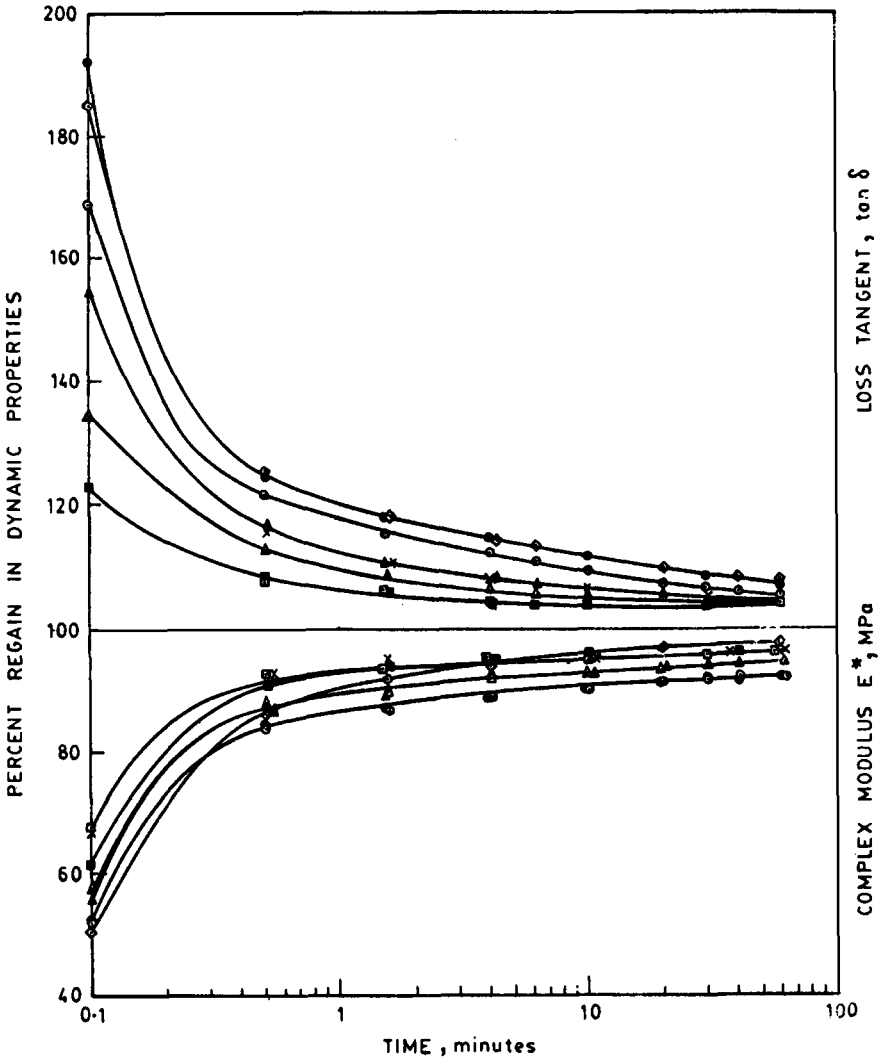

Figure 10 Thixotropic recovery of the dynamic properties at low amplitude after cycling at 5% DSA. Key as Figure 3.

Thixotropic Recovery of the Dynamic Properties

Figure 10 demonstrates the thixotropic recovery of the complex modulus, E^* and tan δ, at low amplitude (0.5% DSA), after cycling of the sample at 5% DSA for 10 min. Percentage recovery of the dynamic parameters with respect to time is shown on the plot. Finer particle size black loaded system (B_{CON}, B_{SAF}, B_{HAF}, etc.) shows higher thixotropic change in properties and delayed recovery.

Dynamic Fatigue Life

The dynamic fatigue life measurement has also been carried out using unnicked dumbbell specimens. Studies have been conducted over an extension ratio from 1.8 to 2.4 at room temperature. Figure 11 shows the logarithmic plot of the fatigue life N of the compositions against strain energy density W. The values of the strain exponent, n have been calculated from the slopes of the curves and are given in Table V. The slopes of the curves for all the carbon black loaded vulcanizates except B_{CON} lie between 3.2 and 3.8. The system B_{CON} and silica filled system B_{SIL} gives n values 1.5 and 6.05, respectively.

The n values for the B_{SAF}, B_{HAF}, B_{FEF}, B_{GPF}, and B_{SRF} filled systems are comparable. However, in absolute terms, the superiority in dynamic fatigue life of finer-particle, and high-structure black filled systems is evident at all strain energy input conditions (Fig. 11). At low strain levels, the silica filled system shows fatigue life equal to that of high-structure low-

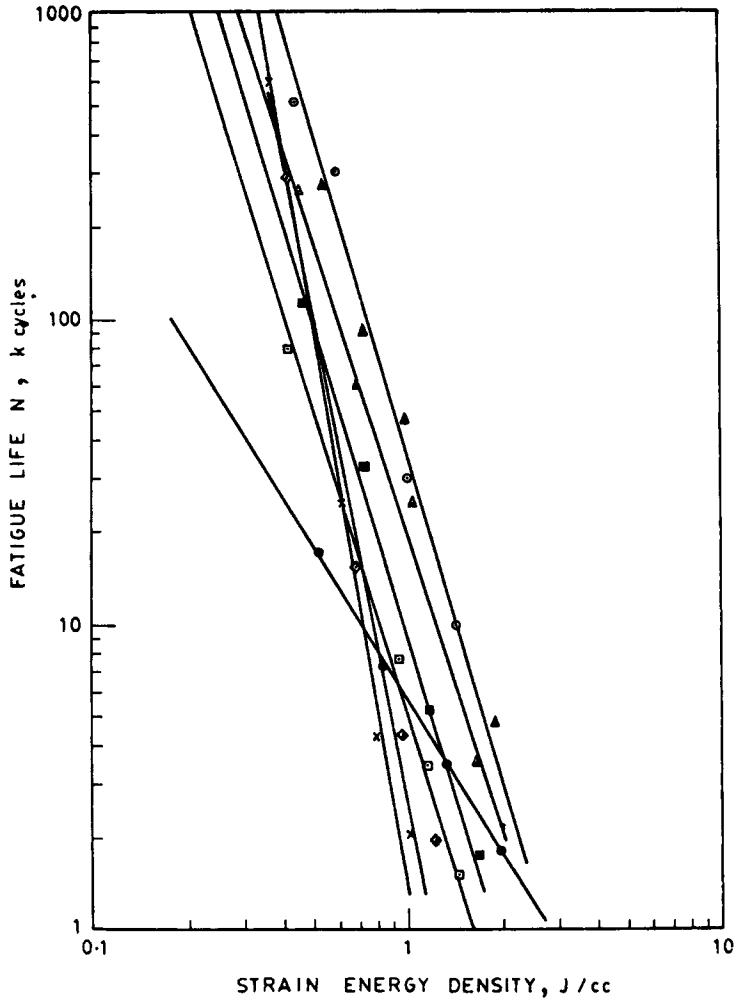

Figure 11 Fatigue life as a function of strain energy. Key as Figure 3.

particle carbon black filled systems. However, at a higher strain level, it has poor fatigue life. In silica–black combined system (B_{SIC}), flex characteristics are more comparable to that of the purely silica filled system (B_{SIL}) than to its black counterpart (B_{HAF}). A profound discrepancy in the conductive black filled system (B_{CON}) with other black loaded systems is observed. It has a strain exponent 1.5. However, at low strain the fatigue life in absolute magnitude is very poor, compared to other systems.

Table V Strain Exponent *n* for Different Vulcanizates

Composition	Strain Exponent (minus)
B_{CON}	1.5
B_{SAF}	3.80
B_{HAF}	3.80
B_{FEF}	3.6
B_{GPF}	3.20
B_{SRF}	3.20
B_{SIC}	5.23
B_{SIL}	6.05

It is important to note that equations 1–3, which were developed from studies of artificially notched vulcanizates, predicts that fatigue life depends on the cut size c_0, the material constant G, and the stored energy density W. In actual practice, however, several other factors such as the nature of the flaw and its interaction with the matrix may impart significant effects on fatigue-to-failure characteristics.

SUMMARY AND CONCLUSIONS

The type and loading of filler has little effect on the molecular relaxation temperatures. An elastomer

having a desirable storage modulus with low sensitivity to temperature change, and better stress–strain properties and fatigue life can be developed by using a filler with a small particle size. However, finer particle size filler loaded systems exhibit pronounced strain dependence, higher thixotropic change, and delayed recovery in dynamic mechanical properties compared to their large particle size counter part. The results also imply that elastic modulus, E', and hysteresis ($\tan \delta$) can be controlled independently through judicious choice of a combination of fillers.

REFERENCES

1. A. R. Payne, in *Reinforcement of Elastomers,* G. Kraus, Ed., Interscience, New York, 1965.
2. A. R. Payne and R. E. Wittaker, *Rubber Chem. Technol.,* **44,** 440 (1971).
3. A. I. Medalia, *Rubber Chem. Technol.,* **46,** 877 (1973).
4. J. D. Ulmer, V. E. Chirico, and C. E. Scott, *Rubber Chem. Technol.,* **46,** 897 (1973).
5. J. D. Ulmer, W. M. Hess, and V. E. Chirico, *Rubber Chem. Technol.,* **47,** 729 (1974).
6. J. M. Caruthers, R. E. Cohen, and A. I. Medalia, *Rubber Chem. Technol.,* **49,** 1076 (1976).
7. J. B. Donnet and A. Voet, *Carbon Black—Physics Chemistry and Elastomer Reinforcement,* Marcel Dekker, New York, 1976.
8. A. I. Medalia, *Rubber Chem. Technol.,* **51,** 437 (1978).
9. Y. Isono and J. D. Ferry, *Rubber Chem. Technol.,* **57,** 925 (1984).
10. N. Nakajima and M. H. Chu, *Rubber Chem. Technol.,* **63,** 110 (1990).
11. A. K. Sircar and T. G. Lamond, *Rubber Chem. Technol.,* **48,** 79 (1975).
12. M. V. Pandey, D. D. Despandey, and V. R. Kapadi, *Int. J. Polym. Mater.,* **12,** 261 (1989).
13. R. G. Stacer, D. M. Husband, and H. L. Stacer, *Rubber Chem. Technol.,* **60,** 227 (1987).
14. J. M. Funt, *Rubber Chem. Technol.,* **61,** 842 (1988).
15. H. Trexler and M. C. H. Lee, *J. Appl. Polym. Sci.,* **32,** 3899 (1986).
16. A. Peterlin, *Ann. Rev. Mater. Sci.,* **2,** 369 (1972).
17. R. S. Rivlin and A. G. Thomas, *J. Polym. Sci.,* **10,** 291 (1953).
18. A. N. Gent, P. B. Lindley, and A. G. Thomas, *J. Appl. Polym. Sci.,* **8,** 455 (1964).
19. G. J. Lake and P. B. Lindley, *J. Appl. Polym. Sci.,* **8,** 707 (1964).
20. E. S. Dizon, A. E. Hicks and V. E. Chirico, *Rubber Chem. Technol.,* **47,** 231 (1974).
21. H. W. Greensmith, *J. Appl. Polym. Sci.,* **7,** 993 (1963).
22. B. Ellis and G. N. Welding, *Rubber Chem. Technol.,* **37,** 571 (1964).
23. H. Smallwood, *Rubber Chem. Technol.,* **18,** 292 (1945).
24. M. C. H. Lee, *Polym. Eng. Sci.,* **25,** 909 (1985).
25. M. C. H. Lee, *J. Appl. Polym. Sci.,* **29,** 499 (1984).
26. J. D. Ferry, *Viscoelastic Properties of Polymer,* John Wiley and Sons, New York, 1970, p. 481.
27. P. P. A. Smit, *Rheol. Acta.,* **5,** 277 (1966).
28. N. K. Dutta and D. K. Tripathy, *Kautsch. Gummi. Kunstst.,* **42,** 665 (1989).
29. S. Fujiwara and K. Fujimoto, *J. Macromol. Sci., Chem.,* **A4,** 1119 (1970).
30. S. Kaufman, W. P. Slichter, and D. D. Deirs, Presented at a meeting of the Division of Rubber Chemistry, American Chemical Society, Chicago, Illinois, October 20–23, 1970, abstracted in *Rubber Chem. Technol.,* **44,** 843 (1971).
31. A. R. Payne and W. E. Watson, *Rubber Chem. Technol.,* **36,** 147 (1963).
32. A. Voet and F. R. Cook, *Rubber Chem. Technol.,* **41,** 1215 (1968).

Received January 23, 1991
Accepted May 20, 1991